NUCLEIC ACID THERAPEUTICS
Volume 32, Number 4, 2022
Mary Ann Liebert, Inc.
DOI: 10.1089/nat.2021.0089

Open camera or QR reader and scan code to access this article and other resources online.

Inhomogeneous Diastereomeric Composition of Mongersen Antisense Phosphorothioate Oligonucleotide Preparations and Related Pharmacological Activity Impairment

Lorenzo Arrico,[1,*] Carmine Stolfi,[2,*] Irene Marafini,[2] Giovanni Monteleone,[2] Salvatore Demartis,[3] Salvatore Bellinvia,[3] Francesca Viti,[3] Marie McNulty,[4] Irene Cabani,[5] Anita Falezza,[5] and Lorenzo Di Bari[1]

Mongersen is a 21-mer antisense oligonucleotide designed to downregulate Mothers against decapentaplegic homolog 7 (SMAD7) expression to treat Crohn's disease. Mongersen was manufactured in numerous batches at different scales during several years of clinical development, which all appeared identical, using common physicochemical analytical techniques, while only phosphorous-31 nuclear magnetic resonance (^{31}P-NMR) in solution showed marked differences. Close-up analysis of 27 mongersen batches revealed marked differences in SMAD7 downregulation in a cell-based assay. Principal component analysis of ^{31}P-NMR profiles showed strong correlation with SMAD7 downregulation and, therefore, with pharmacological efficacy *in vitro*. Mongersen contains 20 phosphorothioate (PS) linkages, whose chirality (Rp/Sp) was not controlled during manufacturing. A different diastereomeric composition throughout batches would lead to superimposable analytical data, but to distinct ^{31}P-NMR profiles, as indeed we found. We tentatively suggest that this may be the origin of different biological activity. As similar manifolds are expected for other PS-based oligonucleotides, the protocol described here provides a general method to identify PS chirality issues and a chemometric tool to score each preparation for this elusive feature.

Keywords: Crohn's disease, phosphorothioate, antisense oligonucleotides, ^{31}P-NMR, mongersen

Introduction

Several synthetic oligonucleotides, including antisense oligonucleotides (ASOs) and small interfering RNAs (siRNAs), have recently gained approval as therapeutic agents and many are in clinical development [1–3]. Synthetic oligonucleotides used therapeutically are chemically modified to improve their pharmacokinetic and pharmacodynamic properties [4,5]. The replacement of phosphodiester (PO) with phosphorothioate (PS) linkages was the first chemical modification to be investigated and it is still the most extensively used, in particular, in RNase H-dependent ASOs [1,4,6,7]. In these ASOs, replacement of the PO with PS improves resistance to nucleases and facilitates cellular uptake and bioavailability *in vivo* without significantly impairing hybridization with the target RNA or the posthybridization RNase H activation [1,4,6,8].

However, the PS modification results in a chiral center with either *S*p or *R*p configuration (Fig. 1). Such chiral centers coupled with the other stereogenic elements of the oligonucleotide chain lead to the formation of 2^n diastereomers, with n being the number of PS linkages present in the PS-

[1]Dipartimento di Chimica e Chimica Industriale, Università di Pisa, Pisa, Italy.
[2]Dipartimento di Medicina dei Sistemi, Università di Roma ''Tor Vergata,'' Rome, Italy.
[3]PPM Services SA, Morbio Inferiore, Switzerland.
[4]Nogra Pharma Limited, Dublin, Ireland.
[5]Regulatory Pharma Net s.r.l., Pisa, Italy.
*These authors contributed equally to this study.

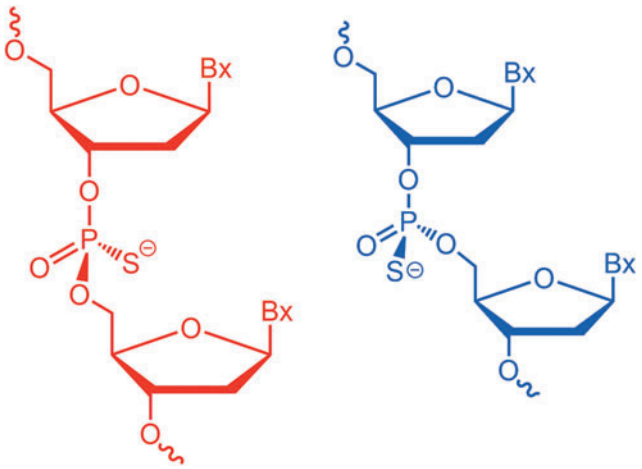

FIG. 1. Schematic representation of phosphorothioate-modified oligonucleotides with *S*p (*red*, *left*) and *R*p (*blue*, *right*) configuration at the phosphorous atom.

modified oligonucleotide [9,10]. Since common synthetic methods of PS-modified oligonucleotides do not allow for control of the chirality at the phosphorous atom, approved PS oligos are a mixture of diastereomers [4].

It has been known for decades that these diastereomers have different biological activity, for example, the two PS nucleotides diastereomers have differential reactivity toward nucleases and kinases, and studies performed with ASOs where the stereochemistry of each PS linkage was predetermined, demonstrated that RNA binding properties, stability of sense/antisense hybrid, and posthybridization mechanisms can be affected by the stereochemistry [9,11–16].

In a study performed to explore the impact of stereochemistry on biological activity, mipomersen, an ASO approved by the Food and Drug Administration to treat homozygous familial hypercholesterolemia, was prepared in sets of *R*p/*S*p sequences across its 19 PS linkages, with the goal of determining the optimal configurations for RNase H1-mediated target cleavage [17]. This analysis demonstrated that the stereochemistry considerably modulates biological activity of the ASO. Stereochemical bias introduced during RNA synthesis has also been shown to impact the biological activity of siRNA [18].

However, as the overall efficacy of an ASO or siRNA is the result of a combination of events, where RNase H1 activity or RNA interference represents only one piece of the mosaic, it has also been reported that ''ASOs with stereorandom PS linkages offer the optimal balance of activity and metabolic stability'' [19], and that controlling PS chirality would not justify the added cost and complexity of the manufacturing process [20].

When stereochemistry is not controlled during oligonucleotide synthesis, random stereochemistry of a PS sequence is not ensured. Internal chiral induction is exerted by the nucleotide sugars and the growing chain itself. The bias toward *R*p or *S*p configurations depends on the conditions of preparation and purification of the ASO, and even small changes in the manufacturing can result in considerable differences in the chiral composition of PS linkages [21,22]. For this reason regulatory authorities require companies that manufacture oligonucleotides for therapeutic use ensure batch-to-batch consistency with regard to diastereomeric composition, which may represent a challenging aspect for most analytical methods, in the presence of a very large number of stereoisomers.

In this study, we focused on mongersen, a 21-mer PS-ASO investigational medicinal product developed for the treatment of Crohn's disease [23–29].

Crohn's disease is a chronic inflammatory bowel disease that affects a considerable portion of the population in Western countries, with increasing annual incidence and prevalence [30]. The Crohn's disease-associated inflammatory process is sustained by defects of normal counter-regulatory mechanisms [31]. One such mechanism involves transforming growth factor-β1 (TGF-β1), a multifunctional cytokine that inhibits multiple inflammatory signals in the gut and that contributes to the maintenance of the mucosal homeostasis [32,33]. In Crohn's disease, the defective activity of TGF-β1 is due to high levels of Mothers against decapentaplegic homolog 7 (SMAD7), an intracellular inhibitor of TGF-β1/SMAD signaling [23].

Consistent with this mechanism, reduction in SMAD7 levels using an ASO targeted to SMAD7 messenger RNA (mRNA) restored TGF-β1 activity, thereby suppressing inflammatory signals in human mucosal cells and in mouse models of colitis [34,35]. These studies paved the way for the development of an oral formulation of the SMAD7-targeted ASO now known as mongersen (previously GED-0301). A total of four phase 1 and phase 2 studies documented highly significant clinical and endoscopic benefit of mongersen in patients with active Crohn's disease [24,25,27,29].

Despite these very positive results, a multicenter randomized double-blind placebo-controlled phase 3 study was prematurely discontinued on the basis of a futility analysis showing that mongersen was not effective in Crohn's disease patients [28]. The reasons for the failure of the phase 3 study, despite the previous clinical trials documenting the efficacy of the drug, have not been addressed.

Mongersen has been prepared in numerous batches during several years of clinical development and, as is the case for most clinically evaluated PS-ASOs, it was synthesized without controlling PS stereochemistry. We had the unique opportunity to analyze samples from each batch to identify unpredicted and undesirable inhomogeneities, which are likely to affect other therapeutic oligonucleotides that contain PS linkages. From this point of view, mongersen constitutes a study case that represents a general situation.

Very recently, upon testing of a limited number of mongersen batches, Marafini *et al.* reported remarkable differences in their pharmacological activity [29].

Over the extended period of mongersen production, several conditions changed. The mere difference in manufacture scale can represent a variable, whose fallout on the composition of the mixture of the 2^{20} possible diastereomers is difficult to evaluate. It should be borne in mind that current analytical techniques would fail to resolve and quantify this complex mixture.

With this study, we shall demonstrate that (1) phosphorous-31 nuclear magnetic resonance (^{31}P-NMR) reveals inhomogeneity among the various batches and fingerprints them, (2) principal component analysis (PCA) can immediately group families of ^{31}P-NMR spectra, and (3) the PCA families correlate with different biological activities *in vitro*.

This enables us to rationalize one of the possible causes that could have contributed to the failure of the phase 3 study despite the previous positive scientific and clinical evidence. We tentatively assign this inhomogeneity to a variable diastereomeric composition throughout the different preparations.

The specific case of mongersen sheds light on a problem that is likely to be ubiquitous in the context of PS-modified oligonucleotides and validates a method to recognize it and an analytical target to direct manufacturing.

Materials and Methods

Mongersen samples

Mongersen was chemically synthesized using commercially available synthesizers in a process that included oligonucleotide synthesis on solid support, cleavage of the protected oligonucleotide from the solid support, deprotection, preparative chromatography purification, concentration, desalting, and lyophilization to yield the drug substance. Twenty-seven different batches of mongersen, prepared during the course of several years at different manufacturing scales, were studied (Supplementary Table S1). All batches (excluding E) were manufactured in compliance with current good manufacturing practice between 2008 and 2017.

Most of these batches were used in clinical trials. The exception is sample E, which was manufactured on laboratory scale (0.24 mmol, 150 mg) in 2020. Quality control testing performed at the time of manufacture was in line with standard requirements for ASOs and did not reveal significant chemical differences. The batches had a chemical purity of mean 92.1% ± 0.7%. The impurity profile, mainly represented by oligonucleotide-related impurities, was typical of this class of molecules. Of note, the impurity pattern was consistent across batches, as ascertained by reversed-phase high performance liquid chromatography (RP-HPLC) (Supplementary Fig. S1) and liquid chromatography mass spectrometry (LC-MS) (Supplementary Figs. S2 and S3) analyses. All the samples were stored at −20°C.

Quality and homogeneity in terms of purity and impurities profile were reconfirmed by RP-HPLC on all batches before ^{31}P-NMR and *in vitro* testing performed for this study (Supplementary Fig. S1).

Moreover, representative batches were also characterized using a large array of state-of-the-art techniques aimed at detecting possible differences in the chemical composition and physical properties of the batches (ie, solid-state NMR, X-ray powder diffraction, Fourier transform (FT) infrared spectroscopy, FT-Raman spectroscopy, small-angle X-ray scattering, thermal gravimetric analysis evolved gases analysis, differential scanning calorimetry, dynamic vapor sorption, electronic circular dichroism [ECD], and variable temperature ECD). No significant variability between batches was detected (Supplementary Figs. S4–S15).

In vitro *pharmacology experiments*

The human colorectal cancer cell line HCT-116 was obtained from the American Type Culture Collection and maintained in McCoy's 5A (Lonza) supplemented with 10% fetal bovine serum (FBS) (Euroclone) and 1% penicillin/streptomycin (Lonza), in a 37°C 5% CO_2 fully humidified incubator. The cell line was authenticated by short tandem repeat DNA fingerprinting using the PowerPlex 18D System kit according to the manufacturer's instructions (Promega); the profile matched the known DNA fingerprint. To perform transfection experiments, 1 mL of single-cell suspension (2×10^5 cells/mL) was added per well of six-well culture dishes.

The next day, cells were washed with phosphate buffered saline (PBS) (Lonza) and transfected with different batches of mongersen using Opti-MEM I transfection medium plus Lipofectamine 3000 (Lipo) reagent (Thermo Fisher Scientific) according to the manufacturer's instructions. The transfection was performed in a final volume of 2 mL to result in a 1 μg/mL final concentration of each test item. Cells incubated with Opti-MEM I transfection medium and Lipo only were used as internal control. After 24 h, cells were washed with PBS and cultured with McCoy's 5A supplemented with 10% FBS and antibiotics for further 3 or 24 h to assess SMAD7 RNA transcripts or SMAD7 protein expression, respectively. Cells were then washed with PBS and either RNA or total proteins were extracted to perform reverse transcription-quantitative polymerase chain reaction (RT-qPCR) and Western blotting experiments.

RNA was extracted using PureLink mRNA mini kit (Thermo Fisher Scientific) according to the manufacturer's instructions. A constant amount of RNA (1 μg per sample) was reverse transcribed into complementary DNA (cDNA), and 1 μL of cDNA per sample was then amplified by RT-qPCR using iQ SYBR Green Supermix (Bio-Rad Laboratories, Milan, Italy) and the following primers: SMAD7: forward: 5′-GCCCGACTTCTTCATGGTGT-3′; reverse: 5′-TGCCGCTCCTTCAGTTTCTT-3′, β-actin: forward: 5′-AA GATGACCCAGATCATGTTTGAGACC-3′; reverse: 5′-AGCCAGTCCAGACGCAGGAT-3′. SMAD7 RNA expression was calculated relative to the housekeeping β-actin gene on the base of the ΔΔCt algorithm.

Total proteins were extracted using the following lysis buffer: 10 mmol/L N-2-hydroxyethylpiperazine-N'-2-ethanesulfonic (HEPES) pH 7.9, 1 mmol/L ethylenediaminetetra-acetic acid (EDTA), 60 mmol/L KCl, 0.2% Igepal CA-630, 1 mmol/L sodium fluoride, 10 μg/mL aprotinin, 10 μg/mL leupeptin, 1 mmol/L dithiothreitol (DTT), and 1 mmol/L phenylmethylsulfonyl fluoride (PMSF) (all from Sigma-Aldrich). Proteins were separated on a 10% sodium dodecyl sulfate polyacrylamide gel electrophoresis (SDS-PAGE) gel, and blots were then incubated with a mouse antihuman monoclonal anti-SMAD7 antibody (0.5 μg/mL final dilution; R&D Systems) followed by incubation with a rabbit antimouse antibody conjugated to horseradish peroxidase (1:20,000 final dilution; Dako, Cat. No.: MAB2029).

After analysis for SMAD7, each blot was stripped and incubated with a mouse–antihuman monoclonal β-actin antibody (Sigma-Aldrich) to confirm equal loading of the lanes. Computer-assisted scanning densitometry (Image Lab Software) was used to analyze the intensity of the immunoreactive bands. Each batch of mongersen was tested in at least three independent experiments. Data were analyzed using the Student's *t*-test. Each experiment included the negative control (transfection reagent-only treated cells) and the mongersen reference batch H.

NMR experiments

In all cases, the ASOs were dissolved in D_2O (~9 mg in 0.5 mL) and immediately subjected to NMR (^{31}P and ^{1}H)

analysis. The NMR experiments were conducted on an Agilent Inova 600 spectrometer operating at 14.1 T and at 25.0°C using standard ^{1}H-NMR and ^{31}P-NMR pulse sequences. For ^{1}H-NMR, 128 transients were obtained. For ^{31}P-NMR, 2,000 transients with 3-s relaxation times were obtained. The hydrogen deuterium oxide line width did not exceed 1.3 Hz. A line broadening of 2 Hz was applied to the ^{31}P spectra.

Representative ^{1}H- and ^{31}P-NMR spectra are shown in Supplementary Figs. S16–S19. After recording a spectrum as already specified above, the tube containing sample F was heated to 85°C for 20 min. After this, it was cooled to room temperature again and measured a second time at 25°C; data from this experiment are shown in Supplementary Fig. S20.

^{31}P-NMR PCA

PCA was performed using the freeware Chemometrics Agile Tool (http://www.gruppochemiometria.it/index.php/software/19-download-the-r-based-chemometric-software). All the ^{31}P-NMR spectra were digitized between 53 and 57 ppm (a total of 2,175 points each). The samples C, F, G, H, L, M, Q, S, U, and W were chosen as the training set. To perform the PCA, all the NMR spectra were normalized on the area between 57 and 53 ppm. The data matrix was then prepared by arranging the variables in columns and the samples in rows. The PCA was performed on the data matrix by automatically scaling the intensity values through mean centering by column.

Results

In vitro *pharmacology profile*

To identify differences in the pharmacological profiles of different clinical batches of mongersen drug substance (Supplementary Table S1), the downregulation of SMAD7 protein was tested in cells of the human colorectal cancer cell line HCT-116 treated with mongersen or not. This is a well-established bioassay, shown previously to give reproducible results [36]. Before *in vitro* testing, all samples were analyzed by RP-HPLC, which did not reveal significant differences among batches, confirming the considerable stability of mongersen over several years of storage. The batches differ in their ability to reduce the levels of SMAD7 target protein in cultured cells (Fig. 2a, b).

An *in vitro* arbitrary pharmacology performance score was assigned to the batches based on their capability to downregulate the SMAD7 protein as compared with the capability of a reference batch H. The reference batch consistently reduced SMAD7 levels in this assay [29] and induced clinical remission in patients with active Crohn's disease when formulated as gastroresistant delayed release tablets used in the phase 1 and phase 2 clinical studies [24,25]. The *in vitro* pharmacology performance scores are plotted in Fig. 2c.

A color-coded score was assigned to the batches based on their *in vitro* pharmacology performance: green—good performance, yellow—medium performance, and red—poor performance. In addition, we evaluated the ability of some representative batches (ie, H, Z, K, and S) to affect SMAD7 RNA expression by RT-qPCR. Our data, depicted in Supplementary Fig. S21, clearly show the different capability of the tested batches in downregulating SMAD7 RNA transcripts and are in line with data obtained by Western blotting regarding the modulation of SMAD7 protein levels.

^{31}P-NMR spectra of mongersen batches

After ascertaining that all other analytical data had revealed no differences among the various preparations (see Supplementary Data), all batches of drug substance were analyzed by ^{31}P-NMR. Each phosphorous atom of the PS ASO results in a singlet in the ^{31}P-NMR spectrum in the region between 54 and 56 ppm. The fine structure in this region is due to, among other effects, the distribution of *S*p/*R*p centers along the backbone. Most chemical impurities do not contribute to the ^{31}P spectrum in the narrow chemical shift range of PS linkages and, therefore, the differences can arise from stereochemistry.

Wyrzykiewicz and Cole previously reported that the PS linkage formation is not stereorandom [21]. However, these authors suggested that the overall synthetic process is stereoreproducible. This will be correct, when synthesis is performed under rigorously identical conditions using the same starting materials. However, this may not be the case when synthesis scale differs and when drug substance is prepared over a long time span, during which there may be variations in the manufacturing protocols or in the starting materials. Moreover, owing to the diastereomeric nature of

FIG. 2. **(a)** Western blots for SMAD7 protein expression in cells treated with mongersen from different batches. HCT-116 cells were either incubated with Lipofectamine 3000 only (Lipo) or transfected with the indicated batches of drug substance. Whole-cell extracts were prepared and analyzed for SMAD7 expression by Western blotting. β-actin was used as a loading control. One of at least three representative experiments for each set of samples is shown. **(b)** Quantitative analysis of SMAD7/β-actin protein ratio in total extracts of HCT-116 cells treated as indicated in (**a**), as measured by densitometry scanning of Western blots. Values are expressed in a.u. and are the mean ± SEM of at least three experiments for each set of samples. The *dashed lines* represent the SMAD7/β-actin protein ratio in cells transfected with the reference batch H. ''Lipo'' indicates the negative control, with cells treated with transfection reagent only. Reference batch H versus the indicated mongersen batches, $*P < 0.05$, $**P < 0.01$. **(c)** *In vitro* capability of mongersen batches to downregulate SMAD7 protein expression compared with batch H. An arbitrary pharmacology performance score, defined as the mean percentage difference in SMAD7 protein expression between treatment with the indicated batch and the reference batch H, was assigned to the mongersen batches based on their capability to downregulate the SMAD7 protein. The pharmacology performance of the batches is represented by *colored bars* and is defined as follows: *green*—similar to batch H (efficacy within 20% of H), *yellow*—marginal decrease in performance compared with batch H (decrease in efficacy of 20–40% vs. H); *red*—poor performance (>40% decrease of efficacy compared with H). ''Lipo'' indicates the negative control, with cells treated with transfection reagent only. For each batch, the bar represents the mean of at least three independent experiments. a.u., arbitrary units; HCT-116; SEM, standard error of the mean; SMAD7, Mothers against decapentaplegic homolog 7.

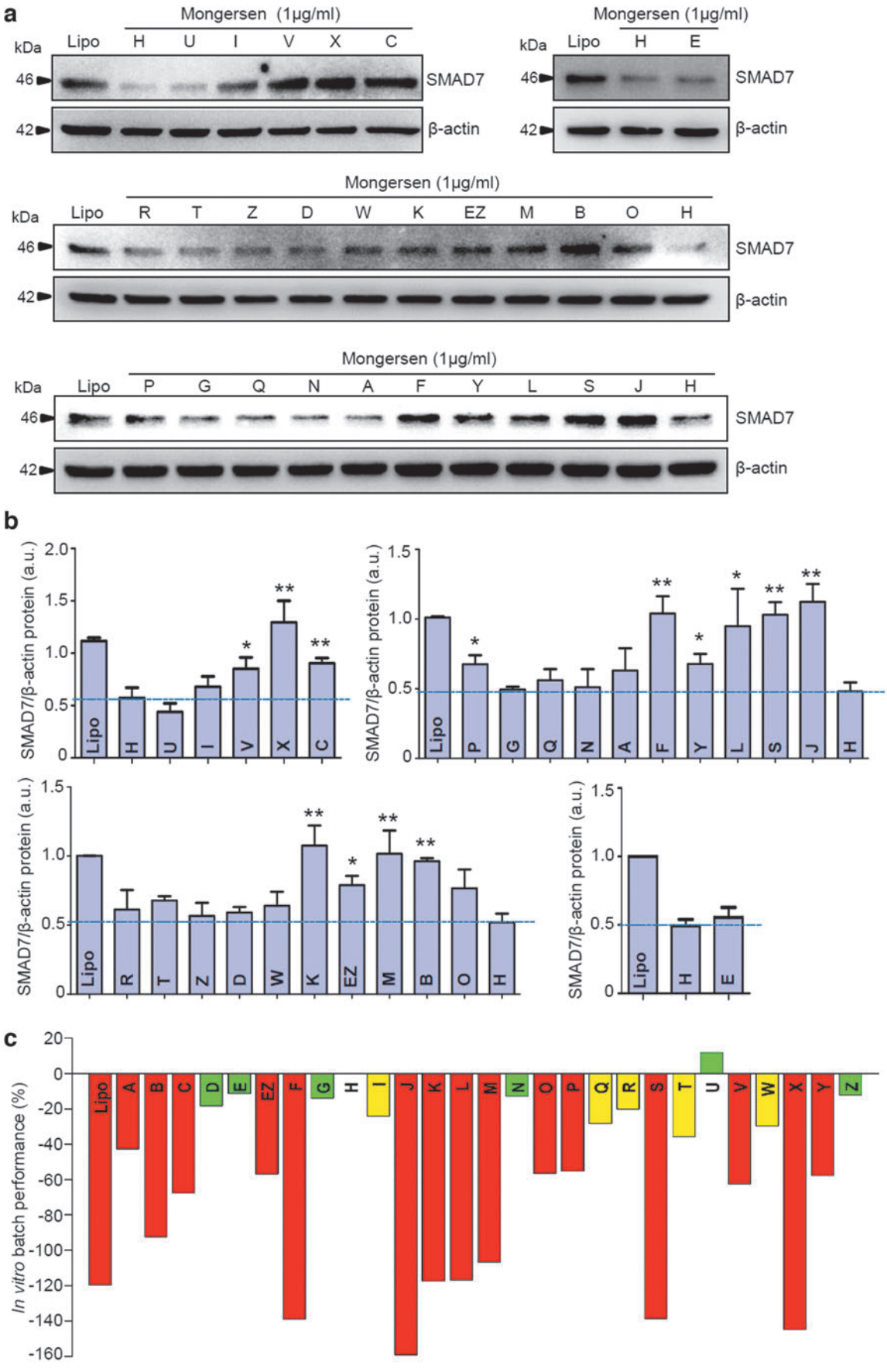
a
Mongersen (1μg/ml)
kDa
Lipo H U I V X C
46
SMAD7
42
β-actin
Mongersen (1μg/ml)
kDa
Lipo H E
46
SMAD7
42
β-actin
Mongersen (1μg/ml)
kDa
Lipo R T Z D W K EZ M B O H
46
SMAD7
42
β-actin
Mongersen (1μg/ml)
kDa
Lipo P G Q N A F Y L S J H
46
SMAD7
42
β-actin
b
SMAD7/β-actin protein (a.u.)
Lipo H U I V X C
Lipo P G Q N A F Y L S J H
Lipo R T Z D W K EZ M B O H
Lipo H E
c
In vitro batch performance (%)
Lipo A B C D E EZ F G H I J K L M N O P Q R S T U V W X Y Z

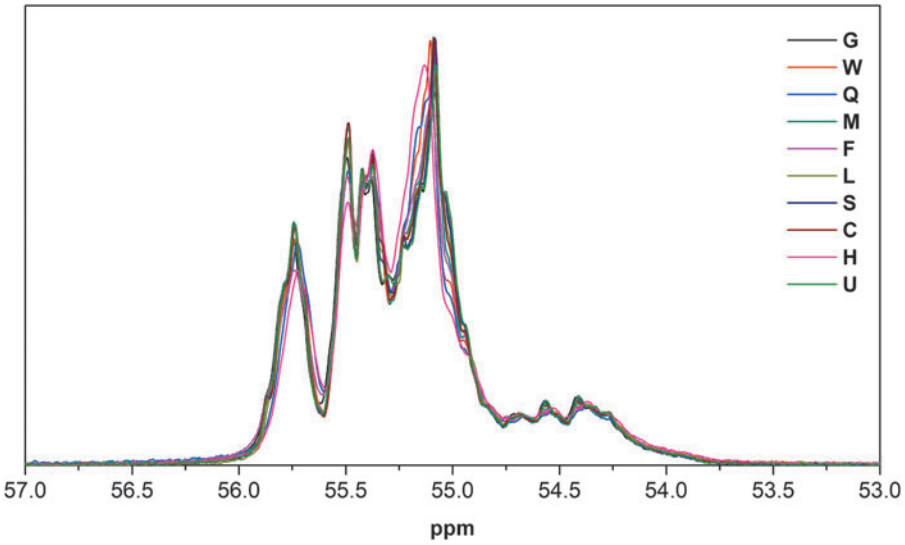

FIG. 3. The ^{31}P-NMR spectra of a subset of mongersen batches, revealing differences in the fine structures of the ^{31}P resonances.

the *Sp*/*Rp* set of isomers, the chromatographic purification steps may further affect this composition [37,38].

Provided the base sequence is the same, a ^{31}P spectrum is further modulated by the sequence of *Sp*/*Rp* at each PS linkages. When there are 20 such linkages, there are 2^{20} possible diastereomers, each leading to a different ^{31}P spectrum. Thus, the signal between 54 and 56 ppm for mongersen batches is complex (we should hypothesize up to $20\times2^{20}=20\times10^{6}$ singlets). For mongersen batches, we observed signals in the ranges of 54.8–55.3, 55.3–55.6, and 55.6–56.0 ppm; signals between 54 and 54.8 ppm were very weak. The fine structures within these regions differed from batch to batch as shown in Fig. 3.

Principal component analysis

Because the ^{31}P spectra are the convolution of a large number of contributions, it was necessary to resort to the application of chemometric analysis. Ten batches were selected that had spectra that appeared to be significantly different from one another (Fig. 3), and spectra of these batches were subjected to PCA using the Chemometric Agile Tool software. Six principal components accounted for >99% of variance of the ^{31}P-NMR spectra, and only two components account for 90% of total variance. The score plot of this training set is shown in Fig. 4 and the scree plot is presented in Supplementary Fig. S22.

The remaining 17 spectra were treated as an external set and were projected onto the score plot of the training set (Fig. 5). Clusters of batches with almost identical PC1/PC2 were distinguished. The batches in the clusters had similar ^{31}P-NMR spectra. A small number of batches are scattered and did not belong to any defined cluster.

Besides the chirality of PS linkages, the ^{31}P spectra would also respond to other stereochemical factors, the most critical one is represented by secondary structures. To exclude that

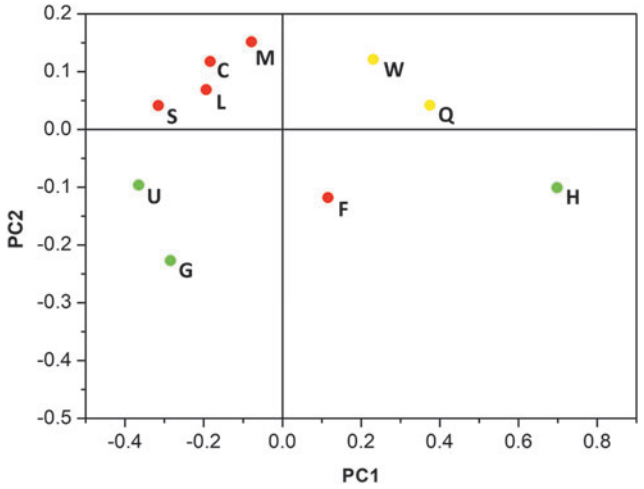

FIG. 4. The score plot of the ^{31}P spectra of the 10 batches of mongersen (M, C, L, S, U, G, W, Q, F, and H) used as a training set for the PCA. PCA, principal component analysis.

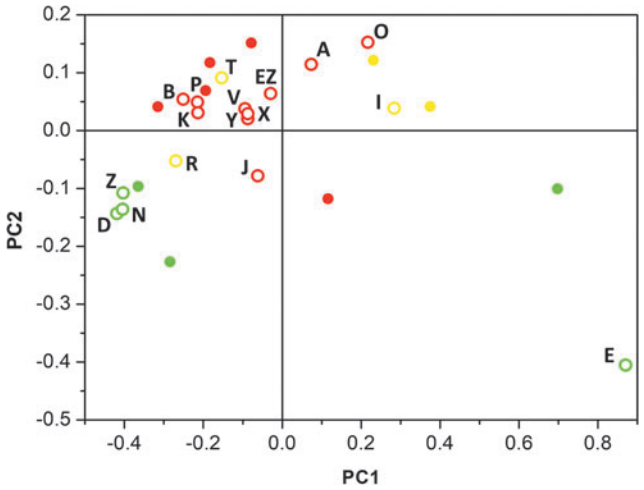

FIG. 5. The score plot of the ^{31}P spectra of the 27 batches of mongersen analyzed in this study. The filled circles (batch number reported in Fig. 4) represent samples from the training set. The *open circles* represent the external set. The *colors correspond* to SMAD7 expression inhibition (as defined in Fig. 2 legend): *green*—similar to batch H, *yellow*—marginal decrease in performance versus H; and *red*—poor performance.

mongersen batches are characterized by different secondary structures, ECD spectra were recorded. All samples had very similar ECD spectra and almost identical ECD versus temperature curves (Supplementary Figs. S14 and S15); all variations were within the experimental error. As a second experiment to exclude other factors, NMR spectra were obtained of batch F before and after heating at 85°C for 20 min. The spectra before and after heat treatment are superimposable (Supplementary Fig. S20), thus the oligonucleotide was not trapped in a folded conformation.

Correlation between SMAD7 inhibition and ^{31}P-NMR PCA

In the score plot of Fig. 5, the cluster of batches centered at (–0.10, 0.05) corresponds to batches that had considerably lower *in vitro* SMAD7 inhibitory effect (''red cluster'') than the reference batch H. Outside this region, there is a transition zone, characterized by data corresponding to batches with marginal decrease in performance compared with batch H. A well-defined area around (–0.35, –0.15) is also distinguishable; in this region, batches with *in vitro* SMAD7 inhibitory performance similar to reference batch H are clustered (''green cluster'').

Two batches located around (0.7, –0.1) and (0.9, –0.45) are batch H (which was the reference for the *in vitro* pharmacology testing, and was the batch manufactured first) and batch E, prepared in 2020 in a laboratory-scale synthesis. Both batches H and E very efficiently inhibited SMAD7 expression in the *in vitro* assay.

Discussion

Mongersen is a PS-ASO designed to downregulate the expression of SMAD7.

Starting in 2008, a total of four phases 1 and 2 clinical studies documented highly significant clinical benefit in active Crohn's disease patients treated with mongersen [24,25,27,29], whereas a phase 3 study was discontinued in 2017 due to lack of efficacy [28].

The *in vitro* assay employing the human cell line HCT-116 provides an excellent model to test the pharmacological activity of this ASO. This assay demonstrated a large degree of variation in the ability of 27 different batches (most of which were used in mongersen clinical studies), to inhibit SMAD7. This variability indicates that there was a lack of reproducibility of the drug substance manufacture, which could not be detected during quality control testing, or by the employment of a large array of state-of-the-art techniques (ie, solid-state NMR, X-ray powder diffraction, FT infrared spectroscopy, FT-Raman spectroscopy, small-angle X-ray scattering, thermal gravimetric analysis, evolved gases analysis, differential scanning calorimetry, dynamic vapor sorption, and LC-MS impurity profiling, or by ECD analysis) aimed at thoroughly characterizing the composition and chemical/physical properties of the batches.

By using these analytical methods, one would have concluded that the product was homogeneous within the batches. It is also worth of note that LC-MS and ^{31}P-NMR itself would reveal the presence of PO impurities. For a number n of PO replacing PS, one would expect an MS peak at mass M-($n \times 16$) and ^{31}P resonances ~ 0 ppm, which can be practically ruled out (below a few percentage of monophosphodiester-related substance detected by LC-MS in all batches) by considering the spectra in Supplementary Figs. S3, S6 and S17.

In contrast, ^{31}P-NMR, which is a selective interrogation tool for the chemical environments of the phosphorous atoms, differed significantly from batch to batch. The remarkable differences in ^{31}P-NMR point to an unexpected manifold, shedding light on the batch-to-batch differences observed in *in vitro* activity.

Of note, the batches of drug substance used in this study were manufactured over the course of several years, and batch size, equipment, parameters, and reagents were changed during this time period.

PCA allowed us to identify clusters of batches with similar ^{31}P-NMR spectra. The spectral characteristics were strongly correlated with *in vitro* activity. Thus, the strategy we describe provides a chemometric tool to highlight similarities and differences in diastereomeric composition of batches of ASO. PC1 and PC2 explained $\sim 90\%$ of total variance of these spectra and were used to provide a two-score characterization of each batch. It can be recognized that there are tight clusters around (–0.35, –0.15) and (–0.10, 0.05), several somewhat scattered points and two outliers (E and H).

These two batches, H and E, were unique with regard to their manufacture: the former is the first clinical batch of drug substance prepared in 2008, and the latter is the result of a very small laboratory-scale preparation from 2020. We can conclude that ^{31}P-NMR in solution fingerprints the stereochemical identity of our specific drug substance mongersen. Noteworthy, preparations with the same ^{31}P spectrum profile behave very similarly in biological assays.

Thus, ^{31}P-NMR/PCA provided an analytical measure that correlated with *in vitro* activity of mongersen.

Among possible explanations of the differential biological activity of mongersen batches, it appeared to us that one matches the experimental observation of variable ^{31}P-NMR profiles in the PS region, in the absence of other evidence of chemical contamination or by-product. Thus, we put forward that the common origin of the variances in pharmacological activity and in ^{31}P-NMR is PS stereochemistry. Unfortunately, it is difficult to corroborate this hypothesis with more stringent experimental data and we leave it to further study and discussion.

This mongersen case study sheds light on a problem that is likely to be ubiquitous in the context of PS-modified oligonucleotides, which could have influenced the drug development of this specific ASO and may affect the future clinical advancement of these medical products.

Conclusions

Using solution ^{31}P-NMR, a commonly available analytical tool, and PCA, we developed a protocol to fingerprint synthesis batches of oligonucleotide drug substance. The observed variation of ^{31}P-NMR in the narrow range of PS resonances may be tentatively assigned to the diastereomeric composition of mongersen in terms of chirality at phosphorous. The ^{31}P-NMR/PCA scores correlate with, and thus may predict, biological activity. We provide evidence that the mongersen batches administered in clinical studies were not homogeneous and presented a different ability to downregulate SMAD7 in cultured cells.

The simple ^{31}P-NMR/PCA protocol described here provides a tool for assessing homogeneity of PS oligonucleotide preparations, particularly where the manufacturing conditions are altered, or where variations in synthetic or purification protocols occur. This tool will be even more valuable in critical situations such as process scale-up or following a change of drug substance manufacturer.

Author Disclosure Statement

M.Mc.N. is an employee of Nogra Pharma Ltd. F.V., S.D., and S.B. are employees of PPM Services SA, Swiss affiliate of Nogra Pharma Ltd. I.C. and A.F. are employees of Regulatory Pharma Net srl (regulatory consultants for the study). G.M., C.S., and L.D.B. have received fees for consultation from PPM Services.

Funding Information

This study was funded by Nogra Pharma Ltd, Dublin, Ireland.

Supplementary Material

Supplementary Data
Supplementary Table S1
Supplementary Figure S1
Supplementary Figure S2
Supplementary Figure S3
Supplementary Figure S4
Supplementary Figure S5
Supplementary Figure S6
Supplementary Figure S7
Supplementary Figure S8
Supplementary Figure S9
Supplementary Figure S10
Supplementary Figure S11
Supplementary Figure S12
Supplementary Figure S13
Supplementary Figure S14
Supplementary Figure S15
Supplementary Figure S16
Supplementary Figure S17
Supplementary Figure S18
Supplementary Figure S19
Supplementary Figure S20
Supplementary Figure S21
Supplementary Figure S22

References

1. Crooke ST, BF Baker, RM Crooke and XH Liang. (2021). Antisense technology: an overview and prospectus. Nat Rev Drug Discov 20:427–453.
2. Roberts TC, R Langer and MJA Wood. (2020). Advances in oligonucleotide drug delivery. Nat Rev Drug Discov 19: 673–694.
3. Crooke ST, JL Witztum, CF Bennett and BF Baker. (2018) RNA-targeted therapeutics. Cell Metabol 27:714–739.
4. Khovarova A and JK Watts. (2017). The chemical evolution of oligonucleotide therapies of clinical utility. Nat Biotechnol 35:238–248.
5. Wan WB and PP Seth. (2016). The medicinal chemistry of therapeutic oligonucleotides. J Med Chem 59:9645–9667.
6. Eckstein F. (2000). Phosphorothioate oligodeoxynucleotides: what is their origin and what is unique about them? Antisense Nucleic Acid Drug Dev 10:117–121.
7. Eckstein F. (2014). Phosphorothioates, essential components of therapeutic oligonucleotides. Nucleic Acid Ther 24:374–387.
8. Kiełpiński LJ, ED Funder, S Schmidt and PH Hagedorn. (2021). Characterization of Escherichia coli RNase H discrimination of DNA phosphorothioate stereoisomers. Nucleic Acid Ther 31:383–391.
9. Eckstein F. (1985). Nucleoside phosphorothioates. Annu Rev Biochem 54:367–402.
10. Eckstein F. (1970). Nucleoside phosphorothioates. J Am Chem Soc 92:4718–4723.
11. Burgers PM, F Eckstein and DH Hunneman. (1979). Stereochemistry of hydrolysis by snake venom phosphodiesterase. J Biol Chem 254:7476–7478.
12. Koziołkiewicz M, A Krakowiak, M Kwinkowski, M Boczkowska and WJ Stec. (1995). Stereodifferentiation—the effect of P chirality of oligo(nucleoside phosphorothioates) on the activity of bacterial RNase H. Nucleic Acids Res 23:5000–5005.
13. Koziołkiewicz M, M Wójcik, A Kobylańska, B Karwowski, B Rębowska, P Guga and WJ Stec. (1997). Stability of stereoregular oligo(nucleoside phosphorothioate)s in human plasma: diastereoselectivity of plasma 3'-exonuclease. Antisense Nucleic Acid Drug Dev 7:43–48.
14. Stec WJ, CS Cierniewski, A Okruszek, A Kobylańska, Z Pawłowska, M Koziołkiewicz, E Pluskota, A Maciaszek, B Rebowska and M Stasiak. (1997). Stereodependent inhibition of plasminogen activator inhibitor type 1 by phosphorothioate oligonucleotides: proof of sequence specificity in cell culture and *in vivo* rat experiments. Antisense Nucleic Acid Drug Dev 7:567–573.
15. Wan WB, MT Migawa, G Vasquez, HM Murray, JG Nichols, H Gaus, A Berdeja, S Lee, CE Hart, *et al.* (2014). Synthesis, biophysical properties and biological activity of second generation antisense oligonucleotides containing chiral phosphorothioate linkages. Nucleic Acids Res 42: 13456–13468.
16. Li M, HL Lightfoot, F Halloy, AL Malinowska, C Berk, A Behera, D Schümperli and J Hall. (2017). Synthesis and cellular activity of stereochemically-pure 2′-O-(2-methoxyethyl)-phosphorothioate oligonucleotides. Chem Commun 53:541–544.
17. Iwamoto N, DCD Butler, N Svrzikapa, S Mohapatra, I Zlatev, DWY Sah, Meena, SM Standley, G Lu, *et al.* (2017). Control of phosphorothioate stereochemistry substantially increases the efficacy of antisense oligonucleotides. Nat Biotechnol 35:845–851.
18. Jahns H, M Roos, J Imig, F Baumann, Y Wang, R Gilmour and J Hall. (2015). Stereochemical bias introduced during RNA synthesis modulates the activity of phosphorothioate siRNAs. Nat Commun 6:6317.
19. Østergaard ME, CL De Hoyos, WB Wan, W Shen, A Low, A Berdeja, G Vasquez, S Murray, MT Migawa, *et al.* (2020). Understanding the effect of controlling phosphorothioate chirality in the DNA gap on the potency and safety of gapmer antisense oligonucleotides. Nucleic Acids Res 48:1691–1700.
20. Crooke ST, PP Seth, TA Vickers and XH Liang. (2020). The interaction of phosphorothioate-containing RNA targeted drugs with proteins is a critical determinant of the therapeutic effects of these agents. J Am Chem Soc 142:14754–14771.

21. Wyrzykiewicz TK and DL Cole. (1995). Stereoreproducibility of the phosphoramidite method in the synthesis of oligonucleotide phosphorothioates. Bioorg Chem 23:33–41.
22. Ravikumar VT and DL Cole. (2002). Development of 2'-O-methoxyethyl phosphorothioate oligonucleotides as antisense drugs under stereochemical control. Org Process Res Dev 6:798–806.
23. Monteleone G, A Kumberova, NM Croft, C McKenzie, HW Steer and TT MacDonald. (2001). Blocking Smad7 restores TGF-β1 signaling in chronic inflammatory bowel disease. J Clin Invest 108:601–609.
24. Monteleone G, MC Fantini, S Onali, F Zorzi, G Sancesario, S Bernardini, E Calabrese, F Viti, I Monteleone, L Biancone and F Pallone. (2012). Phase I clinical trial of Smad7 knockdown using antisense oligonucleotide in patients with active Crohn's disease. Mol Ther 20:870–876.
25. Monteleone G, MF Neurath, S Ardizzone, A Di Sabatino, MC Fantini, F Castiglione, ML Scribano, A Armuzzi, F Caprioli, *et al.* (2015). Mongersen, an oral Smad7 antisense oligonucleotide, and Crohn's disease. N Engl J Med 372: 1104–1113.
26. Monteleone G, A Di Sabatino, S Ardizzone, F Pallone, K Usiskin, X Zhan, G Rossiter and MF Neurath. (2016). Impact of patient characteristics on the clinical efficacy of mongersen (GED-0301), an oral Smad7 antisense oligonucleotide, in active Crohn's disease. Aliment Pharmacol Ther 43:717–724.
27. Feagan BG, BE Sands, G Rossiter, X Li, K Usiskin, X Zhan and JF Colombel. (2018). Effects of mongersen (GED-0301) on endoscopic and clinical outcomes in patients with active Crohn's disease. Gastroenterology 154:61–64
28. Sands BE, BG Feagan, WJ Sandborn, S Schreiber, L Peyrin-Biroulet, JF Colombel, G Rossiter, K Usiskin, S Ather, X Zhan and G D'Haens. (2020). Mongersen (GED-0301) for active Crohn's disease: results of a phase 3 study. Am J Gastroenterol 115:738–745.
29. Marafini I, C Stolfi, E Troncone, E Lolli, S Onali, OA Paoluzi, MC Fantini, L Biancone, E Calabrese, *et al.* (2021). A pharmacological batch of mongersen that downregulates Smad7 is effective as induction therapy in active Crohn's disease: a phase II, open-label study. BioDrugs 35:325–336.
30. Abraham C and JH Cho. (2009). Inflammatory bowel disease. N Engl J Med 361:2066–2078.
31. MacDonald TT, A DiSabatino and JN Gordon. (2005). Immunopathogenesis of Crohn's disease. J Parenter Enter Nutr 29:S118–S125.
32. Feagins LA. (2010). Role of transforming growth factor-β in inflammatory bowel disease and colitis-associated colon cancer. Inflamm Bowel Dis 16:1963–1968.
33. Ihara S, Y Hirata and K Koike. (2017). TGF-β in inflammatory bowel disease: a key regulator of immune cells, epithelium, and the intestinal microbiota. J Gastroenterol 52:777–787.
34. Boirivant M, F Pallone, C Di Giacinto, D Fina, I Monteleone, M Marinaro, R Caruso, A Colantoni, G Palmieri, *et al.* (2006). Inhibition of Smad7 with a specific antisense oligonucleotide facilitates TGF-β1-mediated suppression of colitis. Gastroenterology 131:1786–1798.
35. Garo LP, AK Ajay, M Fujiwara, V Beynon, C Kuhn, G Gabriely, S Sadhukan, R Raheja, S Rubino, HL Weiner and G Murugaiyan (2019). Smad7 controls immunoregulatory PDL2/1-PD1 signaling in intestinal inflammation and autoimmunity. Cell Rep 28:3353–3366.
36. Stolfi C, V De Simone, A Colantoni, E Franzè, E Ribichini, MC Fantini, R Caruso, I Monteleone, GS Sica, *et al.* (2014). A functional role for Smad7 in sustaining colon cancer cell growth and survival. Cell Death Dis 5:e1073.
37. Thayer JR, Y Wu, E Hansen, MD Angelino and S Rao. (2011). Separation of oligonucleotide phosphorothioate diastereoisomers by pellicular anion-exchange chromatography. J Chromatogr A 1218:802–808.
38. Enmark M, M Rova, J Samuelsson, E Örnskov, F Schweikart and T Fornstedt. (2019). Investigation of factors influencing the separation of diastereomers of phosphorothioated oligonucleotides. Anal Bioanal Chem 411:3383–3394.

Address correspondence to:
Lorenzo Di Bari, PhD
Dipartimento di Chimica e Chimica Industriale
Università di Pisa
via Moruzzi 13
Pisa 56124
Italy

E-mail: lorenzo.dibari@unipi.it

Received for publication October 8, 2021; accepted after revision February 3, 2022; Published Online March 9, 2022.